Biological Evaluation, Structure−Activity Relationships, and Three-Dimensional Quantitative Structure−Activity Relationship Studies of Dihydro-β-agarofuran Sesquiterpenes as Modulators of P-Glycoprotein-Dependent Multidrug Resistance

Carolina P. Reyes,[⊥,‡] Francisco Muñoz-Martínez,[⊥,§] Ivan R. Torrecillas,[⊥,#] Cristina R. Mendoza,[‡] Francisco Gamarro,*[,§] Isabel L. Bazzocchi,[‡] Marvin J. Núñez,[†] Leonardo Pardo,[#] Santiago Castanys,[§] Mercedes Campillo,*[,#] and Ignacio A. Jiménez*[,‡]

Instituto Universitario de Bio-Orgánica "Antonio González", Universidad de La Laguna and Instituto Canario de Investigación del Cáncer, Avenida Astrofisico Francisco Sánchez, 2, 38206 La Laguna, Tenerife, Spain, Instituto de Parasitología y Biomedicina "López-Neyra", Consejo Superior de Investigaciones Científicas, Parque Tecnológico de Ciencias de la Salud, Avda. del Conocimiento s/n, 18100 Armilla, Granada, Spain, Laboratori de Medicina Computacional, Unitat de Bioestadistica, Universitat Autònoma de Barcelona, 08193 Cerdanyola del Vallés, Barcelona, Spain, and Departamento de Farmacia y Tecnología Farmacéutica, Facultad de Química y Farmacia, Universidad de El Salvador, Final 25 Avenida Norte, El Salvador

Received March 13, 2007

Multidrug resistance (MDR) is one of the main challenges in the chemotherapy of cancer, malaria, and other important diseases. Here, we report the inhibitory activity of a series of 76 dihydro-β-agarofuran sesquiterpenes, tested on NIH-3T3 cells expressing the human P-glycoprotein (Pgp) multidrug transporter, to establish quantitative comparisons of their respective abilities to block the drug transport activity. The screening was performed on the basis of the ability of sesquiterpenes to modulate the intracellular accumulation of the classical Pgp substrate daunorubicin. To understand the structural basis for inhibitory activity and guide the design of more potent Pgp inhibitors, we have performed a three-dimensional quantitative structure−activity relationship model using the comparative molecular similarity indices analysis (CoMSIA). The most salient features of these requirements are in the region of the substituents at the C-2, C-3, and C-8 positions, which seem to be critical for determining the overall effectiveness of sesquiterpenes as Pgp inhibitors.

Introduction

MDR[a] refers to the phenomenon whereby cancer cells undergoing chemotherapy develop resistance to a number of drugs with very diverse molecular structures and mechanisms of action. It is, thus, a major obstacle in cancer chemotherapy. One of the most important mechanisms of MDR in cancer cells is the overexpression of Pgp and other related drug transporters.[1] Pgp is a plasma membrane-associated, energy-dependent efflux pump that can effectively transport an astonishing variety of anticancer drugs out of the cell. Overexpression of Pgp by tumor cells is an important cause of both intrinsic and acquired resistance to anticancer drugs. Therefore, Pgp is a promising target for cancer therapy, and significant efforts have been focused on the development of effective reversers of the Pgp-mediated MDR.[2]

Natural products have been important sources of new pharmacologically active agents. Plant-derived products have led to the discovery of many clinically useful drugs for the treatment of human diseases, such as antitumor and anti-infective drugs.[3] The sesquiterpene polyesters with a dihydro-β-agarofuran skeleton are the most widespread and characteristic group of secondary metabolites isolated from the *Celastraceae*, which have attracted considerable attention from synthetic organic chemists and pharmacologists due to their complex structures and wide range of biological properties, including MDR reversal agents in cancer cells. On the basis of these properties, sesquiterpenes have been selected as privileged structures.[4,5]

In our program for developing bioactive natural products from the *Celastraceae* as reversal agents of the MDR phenotype, we have recently described the reversal activity of 48 dihydro-β-agarofuran sesquiterpenes[6,7] and elucidated their molecular mechanism of action as Pgp inhibitors.[6,8] Here, we studied by a 96-well microplate-based approach the ability of 76 (**1**−**76**) sesquiterpenes from *Celastraceae* to block the Pgp-mediated daunorubicin (DNR) transport in intact cells. Such high-throughput screening allowed us to determine their K_i values (i.e., the sesquiterpene concentration that yields half-maximal inhibition of Pgp-mediated DNR transport) for the direct comparison of the different potencies of sesquiterpene as Pgp inhibitors. The structural requirements for Pgp inhibition are at present unknown. Thus, these K_i values were also employed to develop a three-dimensional quantitative structure−activity relationship (3D-QSAR)[9] model using an extension of the comparative molecular field analysis (CoMFA) methodology:[10,11] the comparative molecular similarity indices analysis (CoMSIA),[12] to understand the structural elements of this sesquiterpene series that are key for Pgp inhibition. This is accomplished through the ability of CoMFA to represent the 3D-QSAR model in terms of color contour maps that depict locations on this sesquiterpene series where structural modifications might enhance their biological activity. These maps can

* To whom correspondence should be addressed. I. A. Jiménez: Tel.: +34922318594. Fax: 34922318571. E-mail: ignadiaz@ull.es. F. Gamarro: Tel.: +34958181667. Fax: +34958181632. E-mail: gamarro@ipb.csic.es. M. Campillo: Tel.: +34935812348. Fax: +34935812344. E-mail: Mercedes.Campillo@uab.es.

⊥ The authors contributed equally to this work.

‡ Universidad de La Laguna and Instituto Canario de Investigación del Cáncer.

§ Instituto de Parasitología y Biomedicina "López-Neyra".

Universitat Autònoma de Barcelona.

† Universidad de El Salvador.

[a] Abbreviations: SAR, structure−activity relationships; 3D-QSAR, three-dimensional quantitative structure−activity relationships; CoMFA, comparative molecular field analysis; CoMSIA, comparative molecular similarity indices analysis; K_i, inhibition constant; ΔG_{solv}, solvation free energies; log*P*, partition coefficient; PLS, partial least squares; LOO, leave-one-out; RG, random group; I_{max}, maximal inhibition; MDR, multidrug resistance; Pgp, P-glycoprotein; DNR, daunorubicin; TMDs, transmembrane domains; NIH-3T3 MDR1 cells, NIH-3T3 cells transfected with human MDR1 gene which encodes the wild-type (G185) P-glycoprotein multidrug efflux pump; ABC, ATP binding cassette.

10.1021/jm070290v CCC: $37.00
Published on Web 09/12/2007

serve as a guide for designing analogues within the same series of compounds.

Materials and Methods

Cell Cultures and Chemicals. NIH-3T3 cells transfected with human MDR1 gene, which encodes the wild-type (G185) Pgp multidrug efflux pump (NIH-3T3 MDR1 cells), were cultured as described previously.[7] GF120918 was from GlaxoSmithKline. DNR was from Pfizer. Compounds **1**−**76** were obtained from eight *Celastraceae* species or by standard synthetic methods from isolated sesquiterpenes. Compounds **1**−**6**, **8**, **10**, **32**, and **33** were isolated from *Maytenus cuzcoina*;[13] compounds **34** and **35** from *Euonymus europaeus*;[14] compounds **36**−**37**, **41**−**45**, **53**−**60**, **62**, and **66**−**68** from *Zinowiewia costaricensis*;[7] compounds **38**[15] and **50**−**52** from *Crossopetalum urogoga*; compounds **39** from *Maytenus chubutensis*;[16] compounds **40**, **46**−**47**, **64**−**65**, and **70**−**76** from *Maytenus magellanica*;[16] compounds **48** and **49** from *Maytenus canariensis*;[17,18] compounds **61** and **63** from *Maytenus chiapiensis*.[19] Synthetic derivatives **7**, **9**, **11**−**31**,[20] and **69**[7] were prepared from compounds **3**, **8**, **1**, **2**, **4**, and **68** (Figure 1).

3D-QSAR/CoMSIA Method. A preliminary conformational analysis of each compound was performed using the CHARMm-like force field as implemented in Catalyst (Accelrys Software, Inc., San Diego, CA). The best conformer generation option, up to 250 maximum conformers, with a 15 kcal/mol energy cutoff was employed. The five conformers with predicted lower energy were, additionally, fully optimized at the HF/3-21G level of theory. The lowest ab initio energy conformer was selected for developing the 3D-QSAR model.

A critical step in CoMSIA is to select a proper alignment rule. The entire set of sesquiterpene analogues was oriented in space by superimposing the common and rigid dihydro-β-agarofuran skeleton. The K_i values for human Pgp inhibition are a function of both the stabilization of the complexes between the ligand molecules and the protein receptor and the solvation energy of the ligands and their lipophilicity. Thus, the QSAR spreadsheet consists of the logarithmic values of the inhibition constant pK_i (dependent variable), the electrostatic, steric, hydrophobic, and hydrogen donor and hydrogen acceptor fields (independent variables) to mimic the stabilization energy of the receptor−ligand complex, the solvation energy, and the partition coefficient (independent variables). The atom-centered atomic charges used in CoMSIA to evaluate the electrostatic contributions were computed from the molecular electrostatic potential[21] using 6-31G* basis set, which is a common procedure for the simulation of proteins, nucleic acids, and organic molecules.[22] Solvation free energies (ΔG_{solv}) of sesquiterpenes were calculated with the PM3-SR5.42R procedure within the AMSOL 6.7.2 program.[23] The potential fields were calculated at each lattice intersection of a regularly spaced grid of 2 Å. An sp^3 carbon atom with a van der Waals radius of 1.52 Å carrying a charge of +1.0 served as a probe atom to calculated the fields with an attenuation factor of 0.3.[24] Partial least-squares (PLS) analysis[25−28] was used to derive linear equations from the resulting matrices. Both leave-one-out (LOO) and random group (RG) cross-validation procedures were employed to calculate the cross-validated statistics and to select the number of principal components. The final CoMSIA model was generated using noncross-validation and using the number of components suggested by the cross-validation procedures.

The 3D-QSAR/CoMSIA study was carried out with the QSAR module of the SYBYL 7.3 program,[29] using default parameters. All the quantum mechanical calculations were performed with the Gaussian 98 system of programs.[30]

Modulation of DNR Efflux in NIH-3T3 MDR1 Cells by Sesquiterpenes. We performed the screening of sesquiterpenes by the microplate-based procedure described in our previous work,[7] which briefly consist in plating NIH-3T3 MDR1 cells in 96-well plates the day before the experiment at a density of 2×10^4 cells per well. The resulting cell monolayers were incubated with DNR 10 μM for 2 h at 37 °C in the presence of increasing concentrations of sesquiterpene to generate concentration-dependent DNR accumulation curves. After the incubation period, the cells were extensively washed prior to adding 50 μL/well of lysis buffer (Tris-HCl 20 mM pH 7.4, SDS 0.2%) to release the DNR accumulated inside the cells. Finally, the fluorescence due to DNR ($\lambda_{excitation}$ = 480 nm; $\lambda_{emission}$ = 590 nm) was measured in a microplate spectrofluorometer "SpectraMax Gemini EM" (Molecular Devices, Sunnyvale, CA) using the SoftmaxPro 4.3 software (also from Molecular Devices). To calculate the K_i for the inhibition of DNR efflux, data points obtained at increasing concentrations of sesquiterpenes were normalized considering the value of 100% Pgp inhibition such obtained when incubating the cells in the presence of 2 μM of the third-generation Pgp inhibitor GF120918. Normalized data points were plotted and fitted to the Hill equation for allosteric interactions, using SigmaPlot2000 software: $i = (I_{max} \times S^n)/(K_i + S^n)$; where i is the inhibition of DNR efflux at a given sesquiterpene concentration, I_{max} is the maximal inhibition (100% Pgp inhibition in the presence of GF120918), S is the concentration of sesquiterpene, and n is the Hill coefficient, which determines the sigmoidicity of the curve. We noticed that GF120918 yielded some level of intrinsic fluorescence at the wavelengths used to measure DNR fluorescence, which could contribute to overestimate the real value of maximal DNR accumulation and, thus, diminishing the real I_{max} of sesquiterpenes. Therefore, we subtracted the intrinsic fluorescence due to GF120918 in the control of Pgp maximal inhibition.

Results and Discussion

Chemistry. Repeated chromatography of the *n*-hexane/Et_2O (1:1) extract of the fruits of *Maytenus cuzcoina* on Sephadex LH-20 and silica gel yielded the new sesquiterpene **8**, along with the known sesquiterpenes **1**−**6**, **10**, **32**, and **33**, and repeated chromatography of the CH_2Cl_2 extract of the leaves of *Crossopetalum uragoga* yielded, in addition to the known compound **38**, the new compounds **50**−**52** (Figure 1).

Compound **8** showed the molecular formula $C_{27}H_{32}O_{11}$ by HREIMS, ^1H, and ^{13}C NMR spectroscopic studies. The IR spectrum showed absorption bands for hydroxyl (3467 cm^{-1}) and ester (1719 cm^{-1}) groups. The EIMS exhibited peaks attributable to the presence of methyl ($M^+ - 15$, *m/z* 517 CH_3), hydroxyl ($M^+ - 15-18$, *m/z* 499, H_2O), acetate ($M^+ - 60$, *m/z* 472, CH_3COOH), and furoate ($M^+ - 15-112$, *m/z* 405, C_4H_3OCOOH) groups. This was confirmed by the ^1H NMR spectrum, which also indicated the presence of signals for one acetyl group at δ 2.06 (3H, s) and six protons in the aromatic region for two furoyl groups at δ 8.17 (1H, s), 8.04 (1H, s), 7.44 (2H, s), 6.83 (1H, d, J = 1.1 Hz), and 6.77 (1H, d, J = 1.1 Hz), which were confirmed by ^{13}C NMR data. In addition, five methine protons at δ 5.64 (1H, s, H-6), 5.25 (1H, m, H-2), 5.01 (1H, d, J = 6.7 Hz, H-9), 4.38 (1H, s, H-1), and 2.35 (1H, s, H-7), and two sets of methylene protons at δ 2.54 (1H, m, H-8α), 2.22 (1H, dd, J = 1.6, 18.4 Hz, H-8β), and 2.02 (2H, m, H-3) were observed. A methyl at δ 1.47 bound to a tertiary carbon at δ 70.1 in the ^{13}C NMR spectrum and signals for three angular methyls, were also observed (Tables 1 and 2). All these data indicate that compound **8** is a pentasubstituted dihydro-β-agarofuran sesquiterpene.

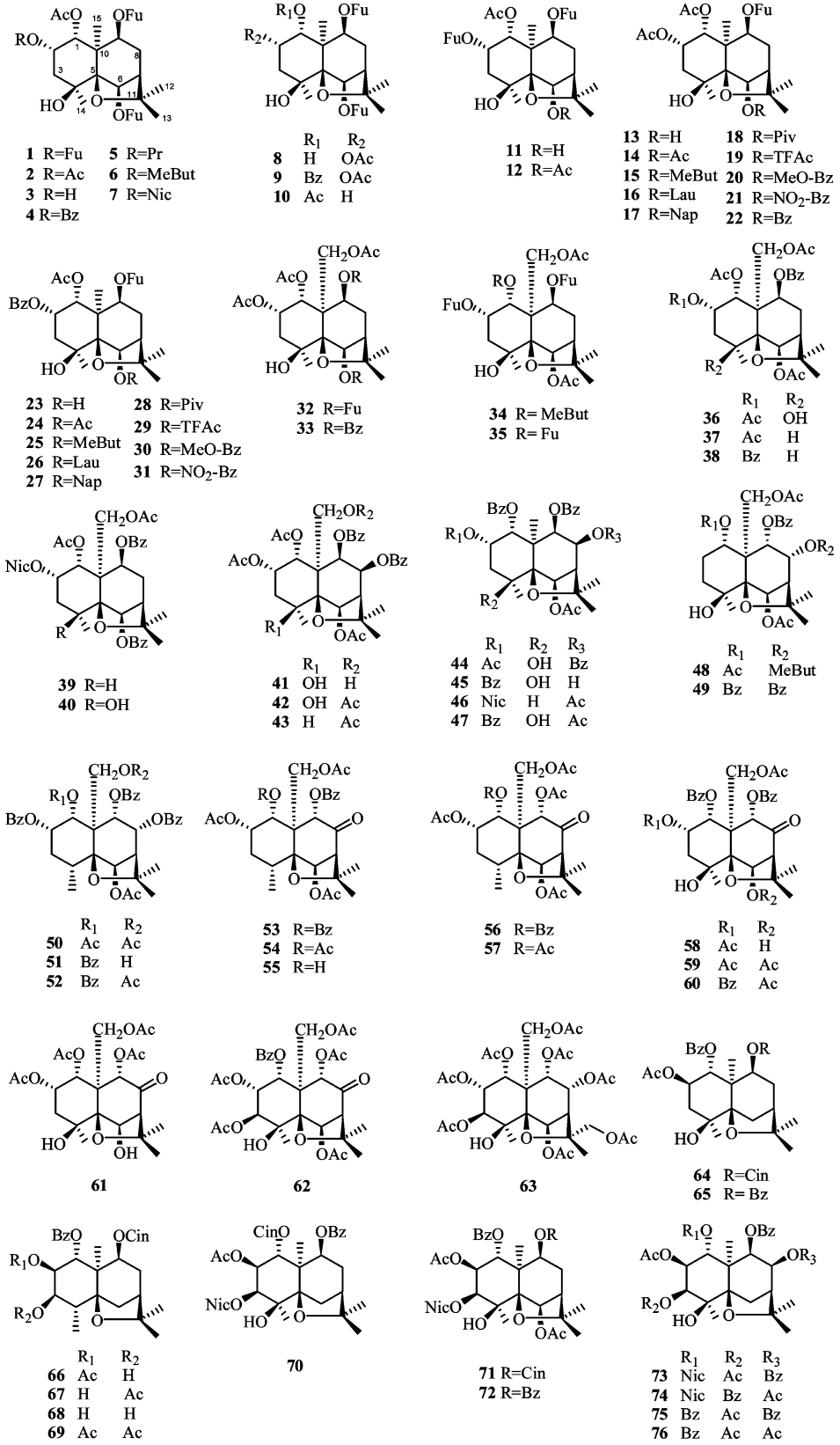

Figure 1. Structure of the sesquiterpenes assayed for the inhibition of the human Pgp.

The relative stereochemistry of **8** was established on the basis of the coupling constants and confirmed by a ROESY experiment, showing ROE effects between H-1 and H-2 and H-3, and between H-15 and H-6 and H-9 and Me-14. The chemical shifts for the carbons attached to protons were assigned according to a 2D heteronuclear HSQC experiment and the already known proton shifts. The regiosubstitution of the ester functions was determined by an HMBC experiment, showing a three-bond correlation between the carboxyl signal of the acetate group at δ_C 171.4 and the signal at δ_H 5.25 (H-2), while the carboxyl signals of the furoate groups at δ_C 161.9 and 162.3 were correlated with the signal at δ_H 5.01 (H-9) and 5.64 (H-6), respectively. The hydroxyl group was located at C-1 because the signal at δ_C 68.1 was correlated with the signals at δ_H 2.02

Table 1. ^{1}H NMR (δ, $CDCl_3$, J in Hz in Parentheses) Data of Compounds **7**−**9**, **38**, and **50**−**52**

	H-1	H-2	H-3	H-4	H-6	H-7	H-8	H-9	H-15
7	5.54 m	5.82 s	2.18 m[a]		5.69 s	2.37 s	2.18,[a] 2.62 m	4.95 d (6.7)	1.62 s[b]
8	4.38 s	5.25 m	2.02 m		5.64 s	2.35 brs	2.22 dd (1.6, 18.4), 2.54 m	5.01 d (6.7)	1.40 s
9	5.67 m[a]	5.67 m[a]	2.06 m		5.67 m[a]	2.36 brs	2.18 dd (1.6, 18.1), 2.56 m	4.99 d (6.8)	1.51 s[b]
38	5.83 d (3.3)	5.88 m	1.97, 2.08 m	2.43 q (7.2)	6.01 s	2.27[a]	2.23, 2.56 m	5.48 d (7.2)	4.43, 5.36 d_{AB} (12.6)
50[c]	6.27 d (4.3)	6.20 m	1.95,[b] 2.50 m	2.27 q (7.8)	7.23 s	2.20 d (3.6)	6.08 m[a]	6.30 d (6.1)	5.09, 6.08[a] d_{AB} (13.3)
51	6.00 d (3.8)	5.77 m	2.05, 2.59 m	2.52 q (7.7)	7.03 s	2.68 d (4.4)	5.94 s[a]	5.94 s[a]	4.56, 5.03 d_{AB} (11.6)
52	6.04 d (4.0)	5.84 m	2.02, 2.67 m	2.46 q (7.7)	6.90 s	2.72 d (3.8)	5.80 dd (3.8, 6.0)	5.89 d (6.0)	4.81, 5.77 d_{AB} (13.2)

[a] Overlapping signals. [b] Interchangeable values. [c] C_6D_6.

Table 2. ^{13}C NMR (75 MHz) Data[a] (δ, $CDCl_3$) of Compounds **8**, **38**, and **50**−**52**

C	8	38	**50**[b]	51	52
C-1	68.1 d	75.1 d	77.8 d	76.7 d	77.4 d
C-2	72.8 d	70.2 d	70.5 d	70.3 d	70.0 d
C-3	42.5 t	30.9 t	32.3 t	31.4 t	31.5 t
C-4	70.1 s	33.0 d	33.6 d	32.9 d	32.8 d
C-5	91.4 s	89.2 s	91.2 s	90.2 s	90.3 s
C-6	79.7 d	78.1 d	75.7 d	75.1 s	74.8 s
C-7	49.1 d	48.8 d	54.5 d	53.3 s	53.5 d
C-8	31.1 t	34.9 t	71.8 d	70.5 d	71.1 d
C-9	72.1 d	69.4 d	73.1 d	73.4 d	72.5 d
C-10	52.6 s	53.2 s	52.3 s	54.5 s	51.5 s
C-11	84.9 s	82.8 s	81.7 s	81.8 s	81.4 s
C-12	29.7 q	30.3 q	30.7 q	30.4 q	30.4 q
C-13	25.8 q	26.0 q	25.1 q	24.7 q	24.7 q
C-14	25.2 q	18.1 q	17.4 q	17.8 q	17.0 q
C-15	20.0 q	66.0 t	62.5 t	60.5 t	61.6 t

[a] Data are based on DEPT, HSQC, and HMBC experiments. [b] C_6D_6.

(H-3) and 1.40 (H-15). The structure of compound **8** was accordingly established as 2α-acetoxy-6β,9β-difuroyloxy-1α,4β-dihydroxy-dihydro-β-agarofuran.

Compound **50** was isolated as a colorless lacquer with the molecular formula $C_{42}H_{44}O_{13}$ (HREIMS). The EIMS contained fragmentation ions, suggesting the presence in the molecule of acetate and benzoate groups. This was confirmed by the ^{1}H NMR spectrum, showing three acetate methyl and fifteen aromatic protons for three benzoyl groups, data that were in accordance with the ^{13}C NMR spectrum. In its ^{1}H NMR spectrum were also observed six methine protons, H-1, H-2, H-4, H-6, H-8, and H-9, two methylene systems, H-3 and H-15, and four methyls (Table 1). All these data indicate that compound **50** is a 1,2,6,8,9,15-hexasubstituted dihydro-β-agarofuran sesquiterpene with three acetate and three benzoate groups. The regiosubstitution was established by the long-range ^{1}H−^{13}C HMBC couplings observed between the H-1, H-6, and H-15 proton resonances and the carboxyl signals of the acetate groups, and the H-2, H-8, and H-9 proton resonances were coupled to the carboxyl signals of the benzoate groups. The relative stereochemistry was determined on the basis of the coupling constants and the ROESY experiment, where ROE interactions were observed between H-6/H-14, H-6/H-15, H-1/H-2, H-1/H-3, H-12/H-8, and H-12/H-9.

Analogously, the structure of compounds **51** and **52** was elucidated by spectral methods (Tables 1 and 2). A detailed study of the NMR spectra indicated that compound **52** is the 15-acetyl derivate of **51**, which was confirmed by chemical correlation.

The detailed ^{1}H and ^{13}C NMR (Tables 1 and 2) assignments of the one known sesquiterpene (**38**),[15] which have not been previously reported, were achieved by 1D and 2D techniques, including DEPT, HMBC, HSQC, COSY, and ROESY.

Compounds **7** and **9** were prepared by treatment of the natural compounds **3** and **8** with nicotinoyl chloride and benzoyl chloride, respectively. The structure of compounds **7** and **9** were elucidated by spectroscopic data. Thus, the ^{1}H NMR spectrum of compound **9** indicated that it is the 1-benzoyl derivative of **8**, because the signal of the H-1 proton shifted from δ 4.38 in **8** to δ 5.67 in **9** (Table 1) and considering the presence of additional aromatic protons of the benzoyl group at δ 7.32 (2H, m), 7.46 (1H, m), and 7.66 (2H, d, J = 7.2 Hz). In the same way, the structure of compound **7** was determined as the 2-nicotinoyl derivative of **3**.

The compounds have the basic polyhydroxy dihydro-β-agarofuran sesquiterpenoid cores of 2α,4β-dihydroxy-celorbicol (**7**−**9**),[31] 3,4-dideoxy-maytol (**38**),[15] and alatol (**50**−**52**).[32]

Biological Evaluation. Sesquiterpenes reverse MDR in NIH-3T3 cells expressing the human Pgp due to their ability to block the drug transport activity of Pgp as we have previously shown.[6,8] Because their potency as inhibitors depends on their affinity for the Pgp drug-binding site, we wanted to determine the molecular features that make a given sesquiterpene suitable for optimal interaction with Pgp. To do so, we performed a systematic screening of a series of 76 dihydro-β-agarofuran sesquiterpenes from *Celastraceae* (Table 3) as Pgp inhibitor and calculated the K_i values, using a fluorescence-based microplate assay for DNR transport inhibition, which allowed us to monitor the accumulation of the probe within intact cells. We select DNR as a suitable Pgp substrate for the drug accumulation experiments because the results obtained with our screening method were far more consistent with the antitumoral drug DNR than with other fluorescent probes like rhodamine 6G or Hoechst 33342 (data not shown). The levels of intracellular accumulation of DNR in NIH-3T3 MDR1 cells were highly dependent on the Pgp activity, which determined that even little variations in the concentration of a Pgp inhibitor rendered wide differences in DNR accumulation. This allowed us the calculation of the K_i values with high accuracy.

Surprisingly, sesquiterpenes **1**−**2**, **4**−**8**, **10**, **13**, **16**−**18**, **20**−**21**, **24**−**25**, **28**, **30**−**50**, **53**, **5**−**60**, **64**−**66**, and **68**−**76** possess I_{max} values in the 70−100% range; whereas sesquiterpenes **3**, **9**, **11**−**12**, **14**−**15**, **19**, **22**−**23**, **26**−**27**, **29**, **51**−**52**, **54**, **61-63**, and **67** possess I_{max} values smaller than 70%. This observation could involve mechanistic differences in the way by which sesquiterpenes interact with the Pgp drug-binding site. We have recently shown that there are at least two different sesquiterpene-binding sites within the transmembrane domains (TMDs) of Pgp:[6] a high- and low-affinity binding sites, related in a complex allosteric manner with other drug-binding sites of the Pgp

Table 3. Experimental and CoMSIA-Predicted pK_i of Pgp-Mediated DNR Transport by Sesquiterpenes (K_i, I_{max}) in NIH-3T3 MDR1 cells,[a] Their Solvation Free Energy (ΔG_{solv}), and the Coefficient of Partition (log$P$)

	pK_i (M)							pK_i (M)					
cmpd	$K_i \pm$ SD[b] (μM)	exp	pred[c]	ΔG_{solv}	log$P$	I_{max}	cmpd	$K_i \pm$ SD[b] (μM)	exp	pred[c]	ΔG_{solv}	log$P$	I_{max}
1	2.19 ± 0.46	5.66	5.72	−15.5	6.5	80.5	**39**	0.71 ± 0.07	6.15	6.11	−16.3	8.4	85.8
2	2.91 ± 0.43	5.54	5.60	−13.7	5.1	95.7	**40**	0.58 ± 0.04	6.24	6.19	−17.2	8.2	100.0
3	4.16 ± 0.21	5.38	5.15[d]	−15.5	4.3	51.8	**41**	7.04 ± 0.33	5.15	5.04	−17.3	6.9	73.0
4	0.70 ± 0.05	6.15	6.11	−14.0	7.1	93.1	**42**	1.74 ± 0.24	5.76	5.76	−17.7	7.6	97.0
5	1.13 ± 0.17	5.95	5.95	−12.8	6.2	100.0	**43**	1.71 ± 0.18	5.77	5.83	−18.3	8.3	86.2
6	0.57 ± 0.06	6.24	5.99	−15.6	6.6	95.5	**44**	0.91 ± 0.08	6.04	6.04	−12.3	9.2	84.9
7	7.42 ± 0.25	5.13	5.72[e]	−15.7	6.1	100.0	**45**	1.21 ± 0.21	5.92	5.88	−12.5	8.4	100.0
8	100.00 ± 1.00	4.00	5.20[e]	−13.4	4.3	100.0	**46**	7.72 ± 2.18	5.11	5.95[e]	−14.0	8.7	92.3
9	3.45 ± 2.15	5.46	5.62[d]	−12.7	7.2	45.3	**47**	11.27 ± 14.38	4.95	6.29[e]	−13.0	9.4	80.7
10	6.61 ± 0.85	5.18	5.19	−11.4	5.3	96.3	**48**	1.83 ± 0.00	5.74	5.76	−12.0	7.0	87.7
11	5.53 ± 0.79	5.26	5.30[d]	−15.7	4.7	41.2	**49**	1.22 ± 0.14	5.91	5.88	−14.7	9.6	100.0
12	4.13 ± 0.03	5.38	5.37[d]	−15.6	5.1	61.7	**50**	33.85 ± 3.46	4.47	6.85[e]	−15.4	10.3	100.0
13	17.48 ± 8.27	4.76	5.21[e]	−13.8	3.4	100.0	**51**	1.30 ± 0.01	5.89	5.78[d]	−16.3	11.5	39.5
14	100.00	4.00		−13.8	3.8		**52**	1.98 ± 1.63	5.70	6.56[d]	−13.6	12.4	29.3
15	2.81 ± 0.01	5.55	5.69[d]	−11.5	5.2	66.0	**53**	1.63 ± 0.25	5.79	5.76	−16.7	8.1	81.6
16	0.80 ± 0.09	6.10	6.12	−11.4	9.1	72.7	**54**	2.54 ± 0.06	5.60	5.34[d]	−18.6	6.1	62.3
17	1.65 ± 0.05	5.78	5.81	−13.4	7.3	91.1	**55**	18.39 ± 5.13	4.74	5.40[e]	−17.6	5.0	91.7
18	0.96 ± 0.07	6.02	5.78	−11.2	5.0	75.2	**56**	5.74 ± 2.87	5.24	5.21	−19.2	6.1	96.4
19	12.08 ± 2.40	4.92	5.63[d]	−10.5	4.1	34.0	**57**	9.83 ± 4.13	5.01	5.01	−17.4	4.0	100.0
20	0.70 ± 0.05	6.15	5.56[e]	−13.8	6.1	85.9	**58**	3.97 ± 0.42	5.40	5.66[f]	−17.4	7.2	74.4
21	4.76 ± 0.59	5.32	5.34	−15.7	5.7	76.8	**59**	3.01 ± 0.12	5.52	5.62	−19.1	7.7	81.1
22	8.94 ± 1.02	5.05	5.71[d]	−12.7	6.1	67.9	**60**	1.03 ± 0.06	5.99	6.01	−17.5	10.0	80.0
23	2.50 ± 0.51	5.60	5.54[d]	−14.2	5.7	68.0	**61**	7.65 ± 2.00	5.12	4.94[d]	−18.4	3.3	39.0
24	2.92 ± 0.16	5.53	5.62	−14.1	6.1	92.7	**62**	6.52 ± 0.81	5.19	5.23[d]	−24.4	6.0	53.9
25	1.00 ± 0.07	6.00	6.02	−11.8	7.5	83.3	**63**	6.97 ± 9.30	5.16	5.62[d]	−18.2	3.6	31.0
26	5.16 ± 3.01	5.29	6.48[d]	−11.7	11.4	29.2	**64**	7.61 ± 0.57	5.12	5.08	−12.6	6.5	100.0
27	4.59 ± 0.87	5.34	6.17[d]	−13.7	9.6	54.8	**65**	7.59 ± 1.11	5.12	5.22	−12.0	6.6	89.8
28	1.04 ± 0.07	5.98	6.16	−11.5	7.3	90.0	**66**	8.46 ± 1.49	5.07	5.03	−12.9	6.3	82.9
29	1.56 ± 0.24	5.81	6.01[d]	−10.7	6.4	53.3	**67**	4.25 ± 1.07	5.37	5.48[d]	−13.1	6.2	63.7
30	1.88 ± 0.11	5.73	5.91	−14.1	8.4	75.8	**68**	6.94 ± 3.64	5.16	5.19	−12.8	6.0	76.6
31	1.79 ± 0.22	5.75	5.69	−16.0	7.9	100.0	**69**	2.72 ± 0.30	5.57	5.58	−12.1	7.4	75.8
32	2.44 ± 0.25	5.61	5.75	−17.1	5.4	76.9	**70**	2.07 ± 0.10	5.68	5.69	−14.9	7.6	95.2
33	1.50 ± 0.08	5.82	6.01§	−16.3	7.3	100.0	**71**	25.04 ± 2.83	4.60	5.28[e]	−17.0	8.0	100.0
34	1.94 ± 0.13	5.71	5.71	−15.9	6.9	91.3	**72**	3.75 ± 0.27	5.43	5.39	−16.5	8.0	98.8
35	4.51 ± 1.17	5.35	5.28	−15.7	6.5	99.4	**73**	1.45 ± 0.33	5.84	5.87	−15.9	7.5	100.0
36	4.39 ± 0.12	5.36	5.46	−16.3	5.0	85.0	**74**	1.36 ± 0.18	5.87	5.90	−16.1	7.8	100.0
37	2.36 ± 0.50	5.63	5.65	−15.1	5.7	80.8	**75**	0.73 ± 0.24	6.14	6.07	−14.2	8.8	98.7
38	0.63 ± 0.05	6.20	6.01[f]	−15.2	7.7	88.0	**76**	1.27 ± 0.08	5.90	5.86	−15.1	6.8	88.7

[a] Screening of sesquiterpenes inhibition Pgp-mediated DNR transport in NIH-3T3 MDR1 cells. The K_i was defined as the concentration of sesquiterpene that produces 50% inhibition of Pgp. K_i values were determined using the equation described in Experimental section: Results are expressed as the mean of 2−3 independent experiments performed in triplicate. [b] The standard deviation SD ($P < 0.001$). [c] A dash indicates that the compound was not included in the CoMSIA analysis. [d] Compound not used in the CoMSIA model because $I_{max} < 70\%$. [e] Compound not used in the CoMSIA model because the residual value was greater than two standard deviations. [f] Compound used to test the CoMSIA model.

multidrug-binding pocket. Given that Pgp is able to recognize ligands with a very diverse structure and to bind them in different ways,[33] it could be possible that different subsets of sesquiterpenes bind to Pgp in subtly different ways. This could explain why several sesquiterpenes behave as "full inhibitors" (with I_{max} values in the 70−100% range) and others as "partial inhibitors" (with I_{max} values less than 70%). Each group of compounds could interact with Pgp at different places within the TMDs.

Structure−Activity Relationships. Structure−activity relationship (SAR) studies of the A-ring of sesquiterpenes suggest that a ester group at the C-2 position seems essential for the inhibition of Pgp activity. Comparison of the inhibitory activity of **1**, **2**, and **4**−**6** versus **3** and **10** [K_i(**1**) = 2.2, K_i(**2**) = 2.9, K_i(**4**) = 0.7, K_i(**5**) = 1.1, K_i(**6**) = 0.6 vs K_i(**3**) = 4.2, K_i(**10**) = 6.6] shows that introduction of the carbonyl group of the ester moiety (OFu, **1**; OAc, **2**; OBz, **4**; OPr, **5**; and OMeBut, **6**), capable of acting as a H-bond acceptor in the H-bond interaction with the receptor, produces higher Pgp inhibition with respect to the presence at the same position of either a hydroxyl group (OH, **3**) or a hydrogen (H, **10**; Table 3). The C-3 position plays also an important role because sesquiterpenes with the OAc substituent at this position (**67**, **69**) are more potent [K_i(**67**) = 4.2 vs K_i(**68**) = 6.9; K_i(**69**) = 2.7 vs K_i(**66**) = 8.5] than the compounds with a hydroxyl group at the same position (**66**, **68**). Similarly, the OBz substituent at the C-8 position (**42**, **43**) causes a higher Pgp-inhibition because the nonsubstituted compounds at the same position (**36**, **37**) are less active [K_i(**42**) = 1.7 vs K_i (**36**) = 4.4; K_i (**43**) = 1.7 vs K_i (**37**) = 2.4].

The regularly observed tertiary hydroxyl group at C-4 does not seem important for the optimal inhibition of Pgp because its presence (**40**, **42**) or absence (**39**, **43**) either causes no significant change [K_i(**39**) = 0.7 vs K_i(**40**) = 0.6; K_i(**43**) = 1.7 vs K_i(**42**) = 1.7] or even worsens (**36**, **59**) the overall activity [K_i(**36**) = 4.4 vs K_i(**37**) = 2.4; K_i(**59**) = 3.0 vs K_i(**53**) = 1.6]. This finding could be extended to other positions in the sesquiterpene scaffold. Compounds with an ester group at positions C-1 (OAc, **2**), C-3 (OAc, **69**), and C-6 (OFu, **1**; OMe−OBz, **20**) are more potent than compounds with a hydroxyl group at the same C-1 (**8**), C-3 (**66**), and C-6 (**11**, **13**) positions [K_i(**2**) = 2.9 vs K_i(**8**) = 100.0; K_i(**69**) = 2.7 vs K_i(**66**) = 8.5; K_i(**1**) = 2.2 vs K_i(**11**) = 5.5; K_i(**20**) = 0.7 vs K_i(**13**) = 17.5].

Clearly, compounds with an ester group have a partition coefficient (log$P$) higher than compounds with a hydroxyl group [log$P$(**2**) = 5.1 vs log$P$(**8**) = 4.3; log$P$(**69**) = 7.4 vs log$P$(**66**) = 6.2; log$P$(**1**) = 6.5 vs log$P$(**11**) = 4.7; log$P$(**20**) = 6.1 vs log$P$(**13**) = 3.4]. This might imply that the high hydrophobicity of these inhibitors is a prerequisite for its functionality, because

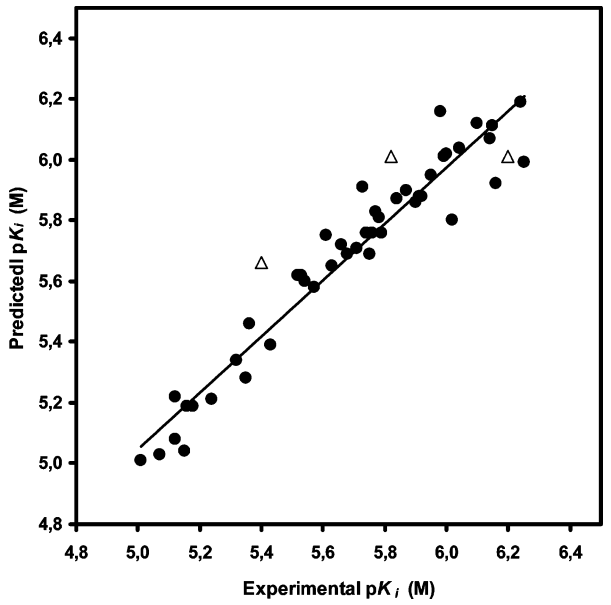

Figure 2. Plot of the predicted versus the experimental values of the inhibition constant (pK_i) for Pgp-mediated DNR transport by applying the CoMSIA model. Ligands **33**, **38**, and **58** (open triangles) were excluded in the CoMSIA model to test its derived predictive values.

they have to be dissolved in the plasma membrane before being able to interact with the Pgp drug-binding site.[34]

On the other hand, the regiosubstitution of the dihydro-β-agarofuran skeleton is an important element for the activity, contributing the substituents at the A-ring more than those at the B-ring. The most active sesquiterpenes as Pgp inhibitors possess a tetra- or penta-substituted 4β-hydroxydihydro-β-agarofuran skeleton.

3D-QSAR/CoMSIA Model. A 3D-QSAR/CoMSIA analysis can only be performed with compounds that bind to the same receptor and act in essentially the same mechanistic manner.[35] Thus, the K_i values determined experimentally for the "full inhibitors" (I_{max} values in the 70−100% range, see above) were related to the independent variables by the PLS methodology (see Methods). Randomly chosen compounds **33**, **38**, and **58** were not included in the training set to test the derived CoMSIA model predictiveness. Compounds **7**, **8**, **13**, **20**, **46**, **47**, **50**, **55**, and **71** were not included because their residual values were greater than two standard deviations. Importantly, these excluded compounds have either extreme values of log*P* (all excluded compounds except **7**, **20**, and **71**); Hill coefficients different from one (**8**, **20**, and **50**, data not shown), and large standard deviations in the experimental K_i values (**13**, **46**−**47**, and **55**). Thus, their mechanism of action or binding mode could be different.[36] Table 4 shows the statistical properties of the model. From a statistical point of view, the obtained values of the LOO and RG cross-validated correlation coefficient ($q^2 = 0.602$ and 0.559, respectively) reveal that the model is a useful tool for predicting the biological activity of these compounds. The theoretically predicted and experimentally determined pK_i values, for the whole set of compounds, are listed in Table 3 and plotted in Figure 2.

Table 4. Statistical Results of K_i Values of the Inhibition of Human Pgp in CoMSIA Models

	K_i
q^{2a}	0.602
q^{2b}	0.559
N^c	8
n^d	45
r^{2e}	0.933
F	62.728
electrostatic[f]	36.4
steric[f]	8.1
H-bond donor[f,g]	11.5
H-bond acceptor[f,g]	13.1
hydrophobicity[f]	15.6
solvation[f]	5.8
log*P*[f]	9.5

[a] LOO correlation coefficient. [b] RGs cross-validation correlation coefficient (five groups). [c] Optimal number of principal components. [d] Number of compounds. [e] Noncross-validated correlation coefficient. [f] Percentage of contribution. [g] On the receptor.

As a further test of robustness, the CoMSIA model was applied to the excluded sesquiterpenes **33**, **38**, and **58**. The theoretically predicted values for these compounds (marked in Table 3) are in agreement with the experimentally determined ones. The relative contributions of the CoMSIA model for the electrostatic, steric, hydrogen bond donor and acceptor on the receptor, hydrophobic, solvation term, and log*P* are shown in Table 4. Figure 3 illustrates the CoMSIA steric (*i*), electrostatic (*ii*), hydrophobic (*iii*), and hydrogen bond donor and acceptor on the receptor (*iv*) maps for the MDR model, using compounds **39** and **75** (white) and **10** and **65** (blue) as reference structures (the color code of the maps is described in the caption).

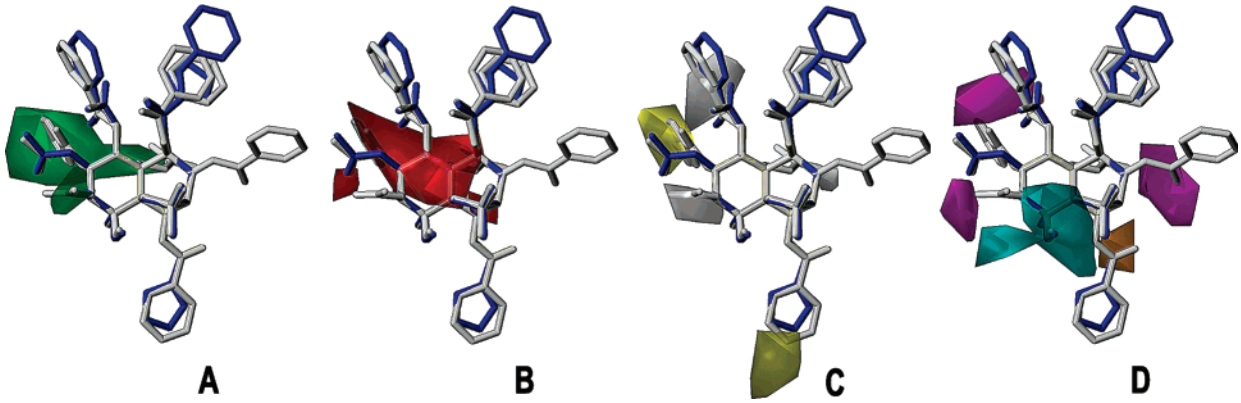

Figure 3. Steric (A), electrostatic (B), hydrophobic (C), and hydrogen bond donor and acceptor (D) maps for Pgp inhibition COMSIA models. Compounds **39** and **75** (white) and **10** and **65** (blue) are shown as reference structures, these being high and low Pgp inhibitors, respectively. The color code is as follows: (A) green and yellow areas depict zones of the space where occupancy by the ligands decreases or increases the K_i values, respectively; (B) areas where a high electron density provided by the ligand decreases (red) the K_i values; (C) yellow and white areas defines regions of space where hydrophobic and hydrophilic groups, respectively, are predicted to decrease K_i; and (D) areas where H-bond donors on the receptor are predicted to enhance (magenta) or decrease (orange) Pgp inhibition, and blue contours show areas where H-bond acceptor zones on the receptor are predicted to increase the K_i values.

The C-2 and C-3 Positions. The steric contour plot (Figure 3A) shows two favorable green areas at the C-2 and C-3 positions, indicating that bulky substituents at these positions increase Pgp inhibition. The bulkier the substituent at C-2, the more efficient is the inhibition (OMeBut, **6** > OBz, **4** > OPr, **5**). The hydrophobic contour map shows a yellow area at the C-2 position and a gray area both at the C-2 and C-3 positions (Figure 3C). Thus, hydrophobic α-substituents at C-2 and hydrophilic β-substituents at both C-2 and C-3 positions (the carbonyl group of the ester moiety, see below) increase Pgp inhibition. The red area in the electrostatic contour map also shows the importance of electronegative groups at these C-2 and C-3 positions for inhibitory activity (Figure 3B). Accordingly, the two magenta regions (in the H-bond donor on the receptor map, Figure 3D) suggest that the electronegative carbonyl group of the ester moiety of the substituents at C-2 and C-3 form a H-bond interaction with the receptor.

The C-4 Position. Cyan regions in the H-bond acceptor on the receptor map (Figure 3D) are present at the C-4 position, indicating that H-bond donor groups, like the hydroxyl group, would decrease Pgp inhibition (see structure−activity relationships section).

The C-6 Position. The importance of the OBz substituent at the C-6 position [K_i(**33**) = 1.5; K_i(**39**) = 0.7; K_i(**40**) = 0.6] is reflected in the yellow area at the bottom of the hydrophobic contour map (Figure 3C). Interestingly, comparison of the inhibitory activity [K_i(**39**) = 0.7 vs K_i(**37**) = 2.4; K_i(**40**) = 0.6 vs K_i(**36**) = 4.4] of **39** and **40** (with ONic and OBz substituents at C-2 and C-6) versus **37** and **36** (with OAc at both positions) shows the importance of bulky aromatic groups at these C-2 and C-6 regions (yellow areas in Figure 3C).

The C-8 Position. The influence of the substituent at the C-8 position is only reflected in the magenta area in the H-bond donor on the receptor map (Figure 3D). Similarly to the C-2 and C-3 positions, the carbonyl group of the OAc (**74**, **76**) or OBz (**42**−**44**, **73**, **75**) substituents is beneficial for Pgp inhibition by forming a H-bond interaction with the receptor.

Conclusions

The ability of cancer cells to develop resistance to cytotoxic drugs is a major barrier to successful chemotherapy. ATP binding cassette (ABC) transporters are involved in the resistance to many cytotoxic drugs. Therefore, the development of inhibitors for these transporters is of high clinical relevance. We have described that natural and semisynthetic dihydro-β-agarofuran sesquiterpenes isolated from *Celastraceae* plants are highly effective, specific reversers of the MDR phenotype in human Pgp-expressing cells, and some of them could be considered as lead compounds for further development of potent and specific MDR reversers. Due to the lack of detailed structural information at the discrete atomic level about the tertiary structure of Pgp, a 3D-QSAR/CoMSIA model has been developed to characterize those structural elements of sesquiterpenes that are keys for the efficient inhibition of Pgp (Figure 4). The most outstanding features are the carbonyl groups at the C-2, C-3, and C-8 positions, which act as a H-bond acceptor in the H-bond interaction with areas of the receptor depicted as pink spheres; a bulky hydrophobic substituent at the C-2β position depicted as a green sphere; and a hydrophobic substituent at the C-6 position depicted as a blue sphere.

In general, the important trends of sesquiterpenes for high inhibitory activity are the overall esterification level of the compounds, the presence of at least two aromati−ester moieties (such as benzoate−nicotinate or benzoate−benzoate), and the size of the molecule. Sesquiterpenes tetra- or penta-substituted show the highest potency, whereas additional esters in the molecule lead to inactive compounds. In contrast to other models,[35] the presence of a basic tertiary nitrogen atom is not essential for Pgp inhibition.

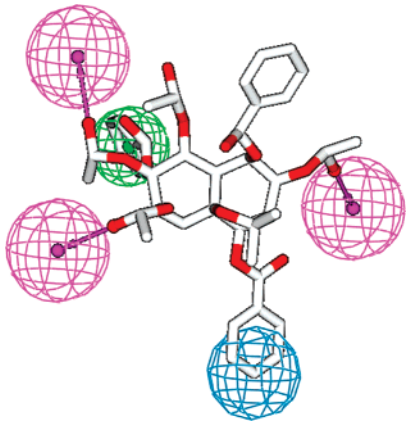

Figure 4. Most outstanding structural elements of the ligands that are keys to high Pgp inhibition obtained with the 3D-QSAR/CoMSIA methodology. Pink spheres represent areas of the receptor that interact with H-bond acceptor moieties of the ligand (i.e., the carbonyl group at the C-2α, C-3, and C-8 positions). The green sphere stands for bulky hydrophobic substituent of the ligand at the C-2β position. The blue region shows the importance of a hydrophobic substituent at the C-6 position of the ligand.

The recently determined structures[37,38] of ABC transporters will contribute in the near future to our understanding of the mechanisms, whereby Pgp recognizes so many different molecules. Weak polar and hydrophobic interactions, through aromatic residues in transmembrane segments of Pgp seem to play an important role in the recognition process.[39,40]

Experimental Section

General Experimental Procedures. Optical rotations were determined on a Perkin-Elmer 241 automatic polarimeter in $CHCl_3$ at 20 °C and the $[\alpha]_D$ are given in 10^{-1} deg cm^2 g^{-1}. UV spectra were obtained on a JASCO V-560 spectrometer in absolute EtOH. IR (film) spectra measured on a Bruker IFS 55 spectrophotometer. ^{1}H and ^{13}C, DEPT, COSY, ROESY, HSQC, and HMBC NMR experiments were performed on a Bruker Avance 400, or a Bruker Avance 300 spectrometer and chemical shifts are shown in δ (ppm) with tetramethylsilane (TMS) as internal reference. EIMS and HREIMS were recorded on a Micromass Autospec spectrometer. Silica gel 60 (15−40 μm) for column chromatography, silica gel 60 F_{254} for TLC, and nanosilica gel 60 F_{254} for preparative HPTLC were purchased from Macherey-Nagel, and Sephadex LH-20 for exclusion chromatography was obtained from Pharmacia Biotech. All the reagents were purchased from Aldrich and used without further purification.

Plant Material. *Maytenus cuzcoina* Loesener (Celastraceae) was collected in December 2000 at Huayllabamba-Urquillos, province of Urubamba, Cusco (Peru). A voucher ("cuz" 02765 A.T. 1004 MO) specimen is deposited in the herbarium of Vargas, Department of Botany, in the National University of San Antonio Abad, Cusco, Peru.

The leaves of *Crossopetalum uragoga* Kuntze was collected in August 1999, in the "El Imposible" National Park, El Salvador. A voucher specimen (JMR-577) was deposited at the Herbarium of the La Laguna Botanic Garden, Santa Tecla, El Salvador.

Extraction and Isolation. The dried fruits of *M. cuzcoina* (250 g) were extracted with *n*-hexane/Et_2O (1:1) in a Soxhlet apparatus. Removal of the solvent under reduced pressure provided 40 g of extract, which was chromatographed on a silica gel column, using increasing polarity mixtures of *n*-hexane−EtOAc as eluant to afford six fractions. In this way, thus, after several chromatographies on

Sephadex LH-20 (*n*-hexane−$CHCl_3$−MeOH, 2:1:1), silica gel (CH_2Cl_2−acetone or CH_2Cl_2−EtOAc of increasing polarity), and preparative HPTLC of the fractions 4 and 5, the known compounds **1**−**6** and **10**,[13] and the new compound **8** (26.0 mg) were isolated. Semisynthetic compounds **7** and **9** were prepared by standard methods.

The dried leaves of *Crossopetalum uragoga* (3.4 kg) were sliced into chips, extracted with EtOH in a Soxhlet apparatus, and concentrated under reduced pressure. The EtOH extract (390.0 g) was partitioned between CH_2Cl_2/H_2O (1:1) to provide CH_2Cl_2 (87.0 g) and H_2O fractions. The CH_2Cl_2 fraction was chromatographed on a silica gel column, using increasing polarity mixtures of *n*-hexane−EtOAc as eluant to afford four fractions. Fractions 2−4 were subjected to column chromatography over Sephadex LH-20 (*n*-hexane−$CHCl_3$−MeOH, 2:1:1) and silica gel (CH_2Cl_2−acetone of increasing polarity). Preparative HPTLC was used to purify the new compounds **50** (63.4 mg), **51** (3.2 mg), and **52** (7.3 mg), in addition to the known compound **38** (45.6 mg).[15]

1α-Acetoxy-6β,9β-difuroyloxy-4β-hydroxy-2α-nicotinoyloxy-dihydro-β-agarofuran (7). A mixture of nicotinoyl chloride (20.0 mg), triethylamine (5 drops), compound **3** (3.5 mg), 4-(dimethylamino)-pyridine (2.0 mg), and imidazole (2.0 m) in dry dichloromethane (2.0 mL) was heated under reflux for16 h. The reaction was quenched by the addition of ethanol (0.5 mL) followed by stirring for 30 min at room temperature. The mixture was evaporated to dryness, and the residue was purified by preparative TLC using CH_2Cl_2/Et_2O (5:1) to give **7** (1.4 mg): colorless lacquer; $[\alpha]^{20}_D$ = +33.6° (*c* 0.14, $CHCl_3$); IR γ_{max} (film) 3423, 2956, 2915, 2847, 1722, 1308, 1284, 1230, 1159, 1023, 761 cm^{-1}; ^1H NMR ($CDCl_3$) δ 1.54 (3H, s), 1.57 (3H, s), 1.60 (3H, s), 1.74 (3H, s, OAc-1), 3,07 (1H, s, OH-4), OFu × 2 [6.75 (1H, s), 6.84 (1H, s), 7.44 (2H, m), 8.04 (1H, s), 8.18 (1H, s)], ONic [7.44 (1H, m), 8.22 (1H, dd, *J* = 1.6, 4.9 Hz), 8.79 (1H, d, *J* = 4.9 Hz), 9.17 (1H, s)], for other signals, see Table 1; MS (EI) *m*/*z* (%) 637 (M^+, 2), 622 (1), 510 (1), 402 (1), 322 (8), 279 (7), 167 (17), 149 (82), 111 (16), 97 (26), 57 (100); HRMS (EI) *m*/*z* calcd for $C_{33}H_{35}NO_{12}$, 637.2159; found, 637.2169.

2α-Acetoxy-6β,9β-difuroyloxy-1α,4β-dihydroxy-dihydro-β-agarofuran (8). Colorless lacquer; $[\alpha]^{20}_D$ = +18.1° (*c* 0.16, $CHCl_3$); UV (EtOH) λ_{max} (log ϵ) 231 (3.8), 220 (3.7) nm; IR γ_{max} (film) 3467, 2956, 2925, 2847, 1719, 1640, 1361, 1310, 1159, 1073, 1025, 877, 760 cm^{-1}; ^1H NMR ($CDCl_3$) δ 1.47 (3H, s, Me-14), 1.53 (3H, s, Me-13), 1.56 (3H, s, Me-12), 2.06 (3H, s, OAc-2), 3.02 (1H, s, OH-4), OFu × 2 [6.77 (1H, d, *J* = 1.1 Hz), 6.83 (1H, d, *J* = 1.1 Hz), 7.44 (2H, s), 8.04 (1H, s), 8.17 (1H, s)], for other signals, see Table 1; ^{13}C NMR ($CDCl_3$) δ OAc-2 [21.3 (q), 171.4 (s)], OFu × 2 [109.8 (2 × d), 119.4 (s) 119.7 (s), 143.9 (d), 144.0 (d), 147.7 (d), 149.1 (d), 161.9 (s, $-CO_2$-9), 162.3 (s, $-CO_2$-6)], for other signals, see Table 2; MS (EI) *m*/*z* (%) 517 (M^+ - CH_3, 2), 499 (1), 472 (1), 422 (2), 405 (3), 360 (3), 342 (2), 248 (5), 230 (4), 173 (4), 149 (4), 95 (100), 77 (5); HRMS (EI) *m*/*z* calcd for $C_{26}H_{29}O_{11}$ ($M^+ - CH_3$), 517.1710; found, 517.1693.

2α-Acetoxy-1α-benzoyloxy-6β,9β-difuroyloxy-4β-hydroxy-dihydro-β-agarofuran (9). A mixture of benzoyl chloride (4 drops), compound **8** (3.4 mg), 4-(dimethylamino)-pyridine (2.0 mg), and imidazole (2.0 m) in dry pyridine (2.0 mL) was heated under reflux for 16 h. The mixture was evaporated to dryness and the residue was dissolved in Et_2O and washed with H_2O, 10% $NaHCO_3$, and brine. The organic layer was stirred over KF (64.0 mg) for 1 h and filtered through celite. The filtrate was dried over anhydrous $MgSO_4$, filtered, and concentrated under reduced pressure. The residue was purified by preparative TLC using CH_2Cl_2/Et_2O (9:1) to give **9** (3.3 mg): colorless lacquer; $[\alpha]^{20}_D$ = +24.7° (*c* 0.17, $CHCl_3$); IR γ_{max} (film) 3442, 2956, 2924, 2846, 1724, 1452, 1270, 1157, 1026, 760, 713 cm^{-1}; ^1H NMR ($CDCl_3$) δ 1.57 (6H, s), 1.69 (3H, s), 2.00 (3H, s, OAc-2), 3.05 (1H, s, OH-4), OFu × 2 [6.50 (1H, s), 6.85 (1H, s), 7.32 (1H, m), 7.46 (1H, m), 7.84 (1H, s), 8.19 (1H, s)], OBz [7.32 (2H, m), 7.46 (1H, m), 7.66 (2H, d, *J* = 7.2 Hz)], for other signals, see Table 1; MS (EI) *m*/*z* (%) 621 ($M^+ - CH_3$, 1), 577 (1), 532 (2), 509 (2), 464 (11), 192 (10), 105 (100), 95 (76); HRMS (EI) *m*/*z* calcd for $C_{33}H_{33}O_{12}$ ($M^+ - CH_3$), 621.1972; found, 621.1957.

1α,6β,15-Triacetoxy-2α-9β-dibenzoyloxy-dihydro-β-agarofuran (38). Colorless lacquer; $[\alpha]^{20}_D$ = +68.2° (*c* 0.11, $CHCl_3$); UV (EtOH) λ_{max} (log ϵ) 231 (4.1), 274 (3.2), 282 (3.1) nm; IR γ_{max} (film) 2922, 2852, 1723, 1458, 1273, 1097, 759 cm^{-1}; ^1H NMR ($CDCl_3$) δ 1.24 (3H, d, *J* = 7.2 Hz, Me-14), 1.44 (3H, s, Me-12), 1.48 (3H, s, Me-13), 1.52 (3H, s, OAc-1), 2.11 (3H, s, OAc-6), 2.27 (3H, s, OAc-15), OBz × 2 [7.51 (6H, m), 8.06 (2H, dd, *J* = 1.2, 7.1 Hz), 8.12 (2H, dd, *J* = 1.4, 7.0 Hz)], for other signals, see Table 1; ^{13}C NMR ($CDCl_3$) δ OAc-15 [20.4 (q), 170.7 (s)], OAc-6 [21.2 (q), 170.0 (s)], OAc-1 [21.3 (q), 169.3 (s)], OBz × 2 [128.3 (2 × d), 128.6 (2 × d), 128.7 (2 × d), 129.1 (s), 129.7 (s), 129.8 (2 × d), 130.1 (d), 133.2 (d), 165.3 (s, $-CO_2$-9), 166.0 (s, $-CO_2$-2)], for other signals, see Table 2; MS (EI) *m*/*z* (%) 621 ($M^+ - CH_3$, 5), 594 (18), 472 (2), 257 (3), 215 (3), 143 (4), 105 (100), 77 (18); HRMS (EI) *m*/*z* calcd for $C_{34}H_{37}O_{11}$ ($M^+ - CH_3$), 621.2336; found, 621.2343.

1α,6β,15-Triacetoxy-2α,8α,9α-tribenzoyloxy-dihydro-β-agarofuran (50). Colorless lacquer; $[\alpha]^{20}_D$ = +5.0° (*c* 0.18, $CHCl_3$); UV (EtOH) λ_{max} (log ϵ) 230 (4.2), 274 (3.1), 282 (3.0) nm; IR γ_{max} (film) 2926, 2853, 1728, 1602, 1452, 1270, 1095, 710 cm^{-1}; ^1H NMR (C_6D_6) δ 1.28 (3H, d, *J* = 7.8 Hz, Me-14), 1.29 (3H, s, Me-12), 1.47 (3H, s, Me-13), 1.51 (3H, s, OAc-6), 1.72 (3H, s, OAc-1), 2.11 (3H, s, OAc-15), OBz × 3 [6.95 (2H, t, *J* = 7.5 Hz), 7.06 (2H, t, *J* = 7.4 Hz), 7.19 (3H, m), 7.32 (2H, t, *J* = 7.5 Hz), 8.14 (2H, dd, *J* = 1.2, 7.2 Hz), 8.42 (2H, m), 8.52 (2H, d, *J* = 7.3 Hz)], for other signals, see Table 1; ^{13}C NMR (C_6D_6) δ OAc-6 [20.7 (q), 170.2 (s)], OAc-1 [21.3 (q), 169.8 (s)], OAc-15 [21.9 (q), 171.2 (s)], OBz × 3 [129.2 (2 × d), 129.3 (2 × d), 129.5 (2 × d), 130.2 (s), 130.3 (s), 130.5 (2 × d), 130.9 (2 × d), 131.1 (2 × d), 131.7 (s), 133.6 (d), 133.8 (d), 133.9 (d), 165.7 (s, $-CO_2$-9), 166.6 (s, $-CO_2$-2), 166.8 (s, $-CO_2$-8)], for other signals, see Table 2; MS (EI) *m*/*z* (%) 756 (M^+, 1), 742 (2), 714 (11), 592 (3), 305 (2), 228 (4), 188 (5), 105 (100), 77 (11); HRMS (EI) *m*/*z* calcd for $C_{42}H_{44}O_{13}$, 756.2782; found, 756.2817.

6β-Acetoxy-1α,2α,8α,9α-tetrabenzoyloxy-15-hydroxy-dihydro-β-agarofuran (51). Colorless lacquer; $[\alpha]^{20}_D$ = −5.6° (*c* 0.09, $CHCl_3$); UV (EtOH) λ_{max} (log ϵ) 228 (3.9), 274 (3.0), 281 (2.8) nm; IR γ_{max} (film) 2924, 2852, 1729, 1601, 1451, 1269, 1093, 708 cm^{-1}; ^1H NMR ($CDCl_3$) δ 1.47 (3H, d, *J* = 7.7 Hz, Me-14), 1.50 (3H, s, Me-12), 1.69 (3H, s, Me-13), 2.15 (3H, s, OAc-6), OBz × 4 [6.82 (2H, t, *J* = 8.0 Hz), 7.03 (2H, t, *J* = 7.9 Hz), 7.13 (1H, t, *J* = 7.6 Hz), 7.30 (1H, t, *J* = 7.6 Hz), 7.50 (10H, m), 7.98 (2H, dd, *J* = 1.4, 7.1 Hz), 8.04 (2H, dd, *J* = 1.4, 7.1 Hz)], for other signals, see Table 1; ^{13}C NMR ($CDCl_3$) δ OAc-6 [21.2 (q), 169.9 (s)], OBz × 4 [127.6 (2 × d), 128.0 (2 × d), 128.6 (2 × d), 128.7 (s), 128.8 (2 × d), 129.0 (s), 129.1 (2 × d), 129.2 (2 × d), 129.4 (s), 129.5 (2 × d), 129.6 (2 × d), 130.0 (s), 132.5 (d), 132.7 (d), 133.1 (d), 133.5 (d), 164.2 (s, $-CO_2$-9), 165.1 (s, $-CO_2$-2), 165.2 (s, $-CO_2$-1), 165.7 (s, $-CO_2$-8)], for other signals, see Table 2; MS (EI) *m*/*z* (%) 776 (M^+, 1), 743 (5), 654 (3), 532 (2), 410 (5), 322 (7), 245 (4), 218 (6), 160 (10), 105 (100), 77 (3); HRMS (EI) *m*/*z* calcd for $C_{45}H_{44}O_{12}$, 776.2833; found, 776.2804.

6β,15-Diacetoxy-1α,2α,8α,9α-tetrabenzoyloxy-dihydro-β-agarofuran (52). Colorless lacquer; $[\alpha]^{20}_D$ = −6.0° (*c* 0.10, $CHCl_3$); UV (EtOH) λ_{max} (log ϵ) 229 (4.2), 274 (3.0), 281 (2.9) nm; IR γ_{max} (film) 2926, 2853, 1729, 1604, 1451, 1270, 1228, 1095, 707 cm^{-1}; ^1H NMR ($CDCl_3$) δ 1.28 (3H, d, *J* = 7.7 Hz, Me-14), 1.53 (3H, s, Me-12), 1.69 (3H, s, Me-13), 1.91 (3H, s, OAc-15), 2.16 (3H, s, OAc-6), OBz × 4 [6.82 (2H, t, *J* = 7.9 Hz), 7.04 (2H, t, *J* = 7.9 Hz), 7.04 (1H, t, *J* = 7.5 Hz), 7.30 (1H, t, *J* = 7.5 Hz), 7.50 (10H, m), 8.01 (2H, dd, *J* = 1.2, 7.2 Hz), 8.06 (2H, dd, *J* = 1.2, 7.2 Hz)], for other signals, see Table 1; ^{13}C NMR ($CDCl_3$) δ OAc-15 [21.2 (q), 171.1 (s)], OAc-6 [21.3 (q), 169.7 (s)], OBz × 4 [127.6 (2 × d), 127.9 (2 × d), 128.3 (2 × d), 128.5 (2 × d), 128.9 (s), 129.1 (s), 129.2 (2 × d), 129.3 (2 × d), 129.4 (s), 129.8 (2 × d), 129.9 (2 × d), 130.2 (s), 132.5 (d), 132.6 (d), 133.2 (d), 133.3 (d), 164.6 (s, $-CO_2$-9), 165.2 (s, $-CO_2$-2), 165.7 (s, $-CO_2$-1), 166.2 (s, $-CO_2$-8)], for other signals, see Table 2; MS (EI) *m*/*z* (%) 803 ($M^+ - CH_3$, 1), 776 (7), 714 (1), 654 (3), 474 (4), 414 (3), 105

(100), 77 (12); HRMS (EI) *m*/*z* calcd for $C_{46}H_{43}O_{13}$ ($M^+ - CH_3$), 803.2704; found, 803.2700.

Acetylation of 51. A mixture of acetic anhydride (2 drops), triethylamine (4 drops), compound **51** (1.5 mg), and 4-(dimethylamino)-pyridine in dichloromethane (2.0 mL) was stirred at room temperature for 16 h. The reaction was quenched by the addition of ethanol (0.5 mL) followed by stirring for 30 min at room temperature. The mixture was evaporated to dryness, and the residue was purified by preparative TLC using *n*-hexane/ethyl acetate (1:1) to give compound **52** (1.0 mg).

Acknowledgment. This work has been supported by the Spanish Grants SAF-2003-04200-C02-01, CTQ-2006-13376/BQU, SAF2004-07103-C02-02, SGR2005-00390, and ICIC (01/2005). We would also like to acknowledge Pharmacia & Upjohn (Barcelona, Spain) for providing the DNR used in this study. C.P.R. thanks to the Gobierno de Canarias for a fellowship.

Supporting Information Available: Experimental data and NMR spectra for the derivatives and the new compounds **7**−**9**, **38**, and **50**−**53**. This material is available free of charge via the Internet at htttp://pubs.acs.org.

References

(1) Gottesman, M. M.; Fojo, T.; Bates, S. E. Multidrug resistance in cancer: Role of ATP-dependent transporters. *Nat. Rev. Cancer* **2002**, *2*, 48−58.
(2) Robert, J.; Jarry, C. Multidrug resistance reversal agents. *J. Med. Chem.* **2003**, *46*, 4805−4817.
(3) Xiao-Tian, L.; Wei-Shou, F. Medicinal chemistry of bioactive natural products; Wiley-Interscience: Hoboken, New Jersey, 2006.
(4) Spivey, A. C.; Weston, M.; Woodhead, S. *Celastraceae* sesquiterpenoids: biological activity and synthesis. *Chem. Soc. Rev.* **2002**, *31*, 43−59.
(5) Cortés-Selva, F.; Jiménez, I. A.; Muñoz-Martìnez, F.; Campillo, M.; Bazzocchi, I. L.; Pardo, L.; Ravelo, A. G.; Castanys, S.; Gamarro, F. Dihydro-*β*-agarofuran sesquiterpenes: A new class of reversal agents of the multidrug-resistant phenotype mediated by P-glycoprotein in the protozoan parasite. *Curr. Pharm. Des.* **2005**, *11*, 3125−3139.
(6) Muñoz-Martìnez, F.; Lu, P.; Cortés-Selva, F.; Pérez-Victoria, J. M.; Jiménez, I. A.; Ravelo, A. G.; Sharom, F. J.; Gamarro, F. Castanys, S. *Celastraceae* sesquiterpenes as a new class of modulators that bind specifically to human P-glycoprotein and reverse cellular multidrug resistance. *Cancer Res.* **2004**, *64*, 7130−7138.
(7) Muñoz-Martìnez, F.; Mendoza, C. R.; Bazzocchi, I. L.; Castanys, S.; Jiménez, I. A.; Gamarro, F. Reversion of human Pgp-dependent multidrug resistance by new sesquiterpenes from *Zinowiewia costaricensis*. *J. Med. Chem.* **2005**, *48*, 4266−4275.
(8) Muñoz-Martínez, F.; Reyes, C. P.; Pérez-Lomas, A. L.; Jiménez, I. A.; Gamarro, F.; Castanys, S. Insights into the molecular mechanism of action of *Celastraceae* sesquiterpenes as specific, non-transported inhibitors of human P-glycoprotein. *Biochim. Biophys. Acta* **2006**, *1758*, 98−110.
(9) Green, S. M.; Marshall, G. R. 3D-QSAR: A current perspective. *Trends Pharmacol. Sci*. **1995**, *16*, 285−291.
(10) Cramer, R. D.; Patterson, D. E.; Bunce, J. D. Comparative molecular field analysis (CoMFA). 1. Effect of shape on binding of steroids to carrier proteins. *J. Am. Chem. Soc.* **1988**, *110*, 5959−5967.
(11) Clark, M.; Cramer, R. D. I.; Jones, D. M.; Patterson, D. E.; Simeroth, P. E. Comparative molecular field analysis (CoMFA). 2. Toward its use with 3D-structural databases. *Tetrahedron Comput. Methodol.* **1990**, *3*, 47−59.
(12) Klebe, G.; Abraham, U.; Mietzner, T. Molecular similarity indices in a comparative analysis (CoMSIA) of drug molecules to correlate and predict their biological activity. *J. Med. Chem.* **1994**, *37*, 4130−4146.
(13) González, A. G.; Tincusi, B. M.; Bazzocchi, I. L.; Tokuda, H.; Nishino, H.; Konoshima, T.; Jiménez, I. A.; Ravelo, A. G. Antitumor promoting effects of sesquiterpenes from *Maytenus cuzcoina* (*Celastraceae*). *Bioorg. Med. Chem.* **2000**, *8*, 1773−1778.
(14) Descoins C., Jr.; Bazzocchi, I. L.; Ravelo, A. G. New sesquiterpenes from *Euonymus europaeus* (*Celastraceae*). *Chem. Pharm. Bull.* **2002**, *50*, 199−202.
(15) Rozsa Z.; Pelczer, I. New Sesquiterpene esters from *Euonymus europaeus* and *E. latifolius*. *J. Chem. Soc., Perkin Trans. 1* **1989**, *6*, 1089−1095.
(16) Kennedy, M. L.; Cortés-Selva, F.; Pérez-Victoria, J. M.; Jiménez, I. A.; González, A. G.; Muñoz, O. M.; Gamarro, F.; Castanys, S.; Ravelo, A. G. Chemosensitization of a multidrug-resistant *Leishmania tropica* line by new sesquiterpenes from *Maytenus magellanica* and *Maytenus chubutensis*. *J. Med. Chem.* **2001**, *44*, 4668−4676.
(17) González, A. G.; Jiménez, I. A.; Ravelo, A. G.; Bazzocchi, I. L. *β*-Agarofuran sesquiterpenes from *Maytenus canariensis*. *Phytochemistry* **1990**, *29*, 2577−2579.
(18) González, A. G.; Jiménez, I. A.; Ravelo, A. G.; Sazatornil, J. G.; Bazzocchi, I. L. New sesquiterpenes with antifeedant activity from *Maytenus canariensis* (*Celastraceae*). *Tetrahedron* **1993**, *49*, 697−702.
(19) Núñez, M. J.; Cortés-Selva, F.; Bazzocchi, I. L.; Jiménez, I. A.; González, A. G.; Ravelo, A. G.; Gavín, J. A. Absolute configuration and complete assignment of ^{13}C NMR data for new sesquiterpenes from *Maytenus chiapensis*. *J. Nat. Prod.* **2003**, *66*, 572−574.
(20) Cortés-Selva, F.; Campillo, M.; Reyes, C. P.; Jiménez, I. A.; Castanys, S.; Bazzocchi, I. L.; Pardo, L.; Gamarro, F.; Ravelo, A. G. SAR Studies of dihydro-*β*-agarofuran sesquiterpenos as inhibitors of the multidrug-resistance phenotype in a *Leishmania tropica* line overexpressing a P-glycoprotein-like transporter. *J. Med. Chem.* **2004**, *47*, 576−587.
(21) Singh, U. C.; Kollman, P. A. An approach to computing electrostatic charges for molecules. *J. Comput. Chem.* **1984**, *5*, 129−145.
(22) Cornell, W. D.; Cieplak, P.; Bayly, C.; Gould, I. R.; Merz, K. M.; Ferguson, D. M.; Spellmeyer, D. C.; Fox, T.; Caldwell, J. W.; Kollman, P. A. A second generation force field for the simulation of proteins, nucleic acids, and organic molecules. *J. Am. Chem. Soc.* **1995**, *117*, 5179−5197.
(23) Hawkins, G. D.; Giesen, D. J.; Lynch, G. C.; Chambers, C. C.; Rossi, I.; Storer, J. W.; Li, J.; Zhu, T.; Winget, P.; Rinaldi, D.; Liotard, D. A.; Cramer, C. J.; Truhlar, D. G. *AMSOL 6.7.2.*; University of Minnesota: Minneapolis, Minnesota, 2002.
(24) Böhm, M.; Stürzebecher, J.; Klebe, G. Three-dimensional quantitative structure-activity relationship analyses using comparative molecular field analysis and comparative molecular similarity indices analysis to elucidate selectivity differences of inhibitors binding to trypsin, thrombin, and factor xa. *J. Med. Chem.* **1999**, *42*, 458−477.
(25) Dunn, W. J. I.; Wold, S.; Edlund, U.; Hellberg, S.; Gasteiger, J. Multivariate structure−activity relationships between data from a battery of biological tests and an ensemble of structure descriptors: the PLS method. *Quant. Struct.-Act. Relat.* **1984**, *3*, 131−137.
(26) Wold, S.; Ruhe, A.; Wold, H.; Dunn, W. J. I. The covariance problem in linear regression. The partial least squares (PLS) approach to generalized inverses. *SIAM J. Sci. Stat. Comput.* **1984**, *5*, 735−743.
(27) Cramer, R. D.; Bunce, J. D.; Patterson, D. E. Crossvalidation, bootstrapping, and partial least squares compared with multiple regression in conventional QSAR studies. *Quant. Struct.-Act. Relat.* **1988**, *7*, 18−25.
(28) Wold, S.; Albano, C.; Dunn, W. J. I.; Edlund, U.; Esbenson, W.; Geladi, P.; Hellberg, S.; Johansson, E.; Lindberg, W.; Sjöström, M. Multivariate data analysis in chemistry. In *Chemometrics: Mathematics and Statistics in Chemistry*; Kowalsky, B. R., Ed.; Reidel: Dordrecht, The Netherlands, 1984; pp 17−95.
(29) *SYBYL 7.3*; Tripos Inc.: 1699 South Hanley Rd., St. Louis, Missouri, 2006.
(30) Frisch, M. J.; Trucks, G. W.; Schlegel, H. B.; Scuseria, G. E.; Robb, M. A.; Cheeseman, J. R.; Zakrzewski, V. G.; Montgomery, J. A., Jr.; Stratmann, R. E.; Burant, J. C.; Dapprich, S.; Millam, J. M.; Daniels, A. D.; Kudin, K. N.; Strain, M. C.; Farkas, O.; Tomasi, J.; Barone, V.; Cossi, M.; Cammi, R.; Mennucci, B.; Pomelli, C.; Adamo, C.; Clifford, S.; Ochterski, J.; Petersson, G. A.; Ayala, P. Y.; Cui, Q.; Morokuma, K.; Malick, D. K.; Rabuck, A. D.; Raghavachari, K.; Foresman, J. B.; Cioslowski, J.; Ortiz, J. V.; Stefanov, B. B.; Liu, G.; Liashenko, A.; Piskorz, P.; Komaromi, I.; Gomperts, R.; Martin, R. L.; Fox, D. J.; Keith, T.; Al-Laham, M. A.; Peng, C. Y.; Nanayakkara, A.; Gonzalez, C.; Challacombe, M.; Gill, P. M. W.; Johnson, B. G.; Chen, W.; Wong, M. W.; Andres, J. L.; Head-Gordon, M.; Replogle, E. S.; Pople, J. A. *Gaussian 98*, revision A.11; Gaussian, Inc.: Pittsburgh, PA, 1998.
(31) Katsuhiro, U.; Naoto, M.; Iwao, M. A sesquiterpene polyester from *Eounymus tanakae*. *Phytochemistry* **1993**, *33*, 230−233.
(32) Kimio, S.; Yoshikazu, S.; Yoshimasa, H.; kiyoyuki, Y. Structure of alatol, a hydrolysis product of a sesquiterpene polyester, alatolin from *Eounymus alatus* forma striatus (thumb.) makimo, and transformation of evoninol to alatol. *Tetrahedrom* **1982**, *38*, 3465−3469.
(33) Loo, T. W.; Clarke, D. M. Location of the rhodamine-binding site in the human multidrug resistance P-glycoprotein. *J. Biol. Chem.* **2002**, *277*, 44332−44338.
(34) Omote, H.; Al-Shawi, M. K. Interaction of transported drugs with the lipid bilayer and P-glycoprotein through a solvation exchange mechanism. *Biophys. J.* **2006**, *90*, 4046−4059.

(35) Pajeva, M.; Wiese, I. K. Structure−activity relationships of multidrug resistance reversers. *Curr. Med. Chem.* **2001**, *8*, 685−713.
(36) Kim, K. H. Outliers in SAR and QSAR: is unusual binding mode a possible source of outliers. *J. Comput.-Aided Mol. Des.* **2007**, *21*, 63−86.
(37) Dawson, R. J.; Locher, K. P. Structure of a bacterial multidrug ABC transporter. *Nature* **2006**, *443*, 180−185.
(38) Locher, K. P.; Lee, A. T.; Rees, D. C. The E. coli BtuCD structure: A framework for ABC transporter architecture and mechanism. *Science* **2002**, *296*, 1091−1098.
(39) Campbell, J. D.; Koike, K.; Moreau, C.; Sansom, M. S. P.; Deeley, R. G.; Cole, S. P. C. Molecular modeling correctly predicts the functional importance of Phe594 in transmembrane helix 11 of the multidrug resistance protein, MRP1 (ABCC1). *J. Biol. Chem.* **2004**, *279*, 463−468.
(40) Pawagi, A. B.; Wang, J.; Silverman, M.; Reithmeier, R. A.; Deber, C. M. Transmembrane aromatic amino acid distribution in P-glycoprotein. A functional role in broad substrate specificity. *J. Mol. Biol.* **1994**, *235*, 554−564.

JM070290V